

# Improved Performance of Magnetrons using the Transparent Cathode<sup>1</sup>

H. Bosman, S. Prasad, M. Fuks, and E. Schamiloglu

*Department of Electrical & Computer Engineering  
MSC01 1100, 1 University of New Mexico  
Albuquerque, NM, 87131, USA*

**Abstract – The transparent cathode is a novel cathode design intended to provide rapid startup in pulsed, relativistic magnetrons [1]. The basic design of the transparent cathode consists of a thin, tubular cathode from which longitudinal strips have been removed. The cathode may also contain a center conductor to provide mechanical support for the cathode strips. The purpose of replacing the traditional solid cylindrical cathode with individual cathode strips is to render the cathode ‘transparent’ to the azimuthal RF electric field. Computer simulations were performed to study the performance of the transparent cathode using the 3D, fully relativistic particle-in-cell code MAGIC. The A6 magnetron geometry [2] was used in the simulations. The output power for the transparent cathode simulation saturates faster than for the solid cathode magnetron. This paper presents a summary of simulation results of this device, and preliminary experimental plans. The use of a transparent cathode in other novel manifestations will also be discussed.**

## 1. Introduction

There is considerable continued interest at improving the output characteristics of existing high power microwave sources and developing new, inexpensive ones. Our recent efforts have been directed at crossed-field devices (with applied radial electric  $E_{0r}$  and axial magnetic  $H_{0z}$  fields) that are capable of generating high power microwaves (HPM), and use coaxial diodes with magnetic insulation (DMI) when the electromagnetic fields are absent. The magnetic insulation in the DMI is provided when the total magnetic field that is tangential to the cathode

$$H_0 = \left( H_{0z}^2 + H_{0\theta}^2 \right)^{1/2} \text{ exceeds its critical value [1]}$$

$$H_{0cr} = \frac{mc^2}{e} \frac{\text{arccosh } \gamma_a}{R_c \ln(R_a/R_c)}, \quad (1)$$

which corresponds to the case where the external boundary of the Brillouin electron flow [2] barely touches the anode surface with radius  $R_a$ . Here  $\gamma_a = 1 + eU/mc^2$ ;  $U$  is the applied voltage;  $R_c$  is a

cathode radius;  $H_{0\theta} = 2I_z/cr$  is the azimuthal magnetic field due to the axial current  $I_z$  of the diode;  $e$  and  $m$  are the charge and rest mass of an electron; and  $c$  is the velocity of light. From (1) it follows that magnetic insulation can be provided without the external axial magnetic field (when  $H_{0z} = 0$ ), that is, with only the field  $H_{0\theta}$ , as is the case in a MILO [3]. However, we will consider devices in which the presence of the axial magnetic field  $H_{0z}$  is necessary to provide synchronous interaction between the electron flow rotating around the cathode with drift velocity

$$v_{e\theta} = c \frac{E_{0r} H_{0z}}{H_0^2}, \quad (2)$$

and one of the eigenmodes of an applied electrodynamic system. The condition of synchronism is

$$v_{e\theta} \approx v_{ph}, \quad (3)$$

where  $v_{ph}$  is the phase velocity of the operating eigenmode.

One way for improving crossed-field devices such as relativistic magnetrons and free electron lasers is through the use of the “transparent” cathode [4,5]. The transparent cathode consists of individual emitters in the form of longitudinal strips periodically arranged on an imaginary cylindrical surface. The strips can be of any cross-section, for example in the form of cylindrical, rectangular, or sectored rods. In this paper we demonstrate the advantages of such cathodes for coaxial devices with applied orthogonal electrostatic and magnetostatic fields through computer simulations with the fully relativistic particle-in-cell code MAGIC [6], together with some preliminary experimental results.

## 2. The Transparent Cathode

The multi-strip cathode is practically transparent for modes that have no axial components of electric field, that is, for TE-modes that are used as operating modes in magnetrons. Due to the penetration of TE-modes inside the transparent cathode, the azimuthal electric field  $E_\theta$  of the operating mode in the electron sheath

<sup>1</sup> The work was supported, in part, by AFOSR.

is much stronger than in the case of a solid metal cathode where  $E_\theta = 0$  on the cathode surface.

In a DMI the electron sheath rotating around the cathode in the crossed fields exists together with the electrons leaving the cathode in the axial direction (leakage current). When a cathode comprises  $N$  individual emitters in the form of longitudinal strips periodically arranged about the cathode radius, electrons leaving such a cathode move in the axial direction as separate streams. The axial current  $I_{Nz}$  along each emitter produces transverse magnetic fields around them (Fig. 1),  $H_{0\perp} = 2I_{Nz}/c\bar{r}$  (here  $\bar{r}$  is radial distance from center of each emitter).

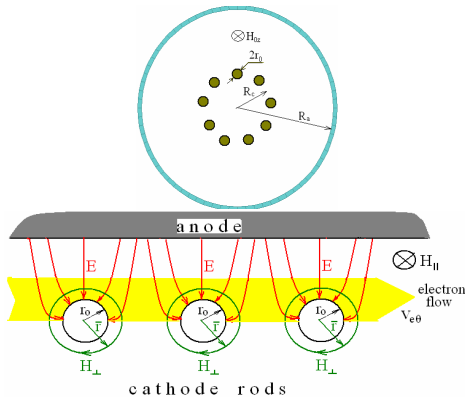


Fig.1. Top: A DMI with a transparent cathode; bottom: periodic magnetic and electric fields near cathode rods in a DMI

The electron sheath, therefore, moves in an additional periodic magnetostatic field produced by the transparent cathode-wiggler. This leads to increasing transverse oscillations in the rotating electron sheath. For magnetrons the periodic magnetic field which promotes faster grouping of electrons provides the same effect as magnetic priming [7] with periodically placed permanent magnets around a resonant system.

The formation of a solid electron sheath around the cathode does not block the currents along cathode strips that produce the periodic magnetic field, as shown in Fig. 2 via computer simulations with the PIC code MAGIC [6] for a DMI with a 6-strip cathode of radius  $R_c = 0.9$  cm and anode with  $R_a = 2.54$  cm when  $U = 0.6$  MV and  $H_{0z} = 10$  kOe.

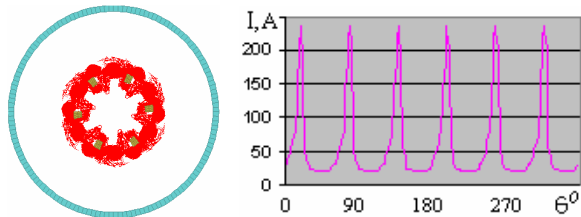


Fig.2. Left: solid electron sheath forming after 2 ns in a DMI for a 1 ns voltage rise time; right: azimuthal distribution of the leakage current after 20 ns

The electrostatic electric field of the applied voltage to the DMI is concentrated on the strips (Fig.1), forming the periodic electrostatic field  $E_w$  of this wiggler (as an example, qualitative distribution of the azimuthal electric field  $E_{w\theta}$  near the cathode as well as distribution of the radial magnetic field  $H_{wr}$  is shown in Fig. 3). Movement of the electron sheath in an additional periodic electrostatic field contributes to the formation of microwave currents as well.

The start time of a magnetron is determined by two factors, each equally important - the noise-level from which the buildup of oscillations starts and the rate of buildup [8]. This situation is related to a magnetron with a solid cathode, in which the initial noise-level is about  $10^{-10}$  of the electric energy of the electron sheath, and the time of development of instability in the symmetrical electron sheath (which is associated with the appearance of microwave current) is several tens of cyclotron periods [2]. Nonuniform emission from a solid cathode through an azimuthally periodic placement of emitting regions (“cathode priming”) was suggested as a way to improve start conditions in a magnetron [9]. The azimuthal modulation in the electron sheath starts almost simultaneously with the start of electron emission, and a suitable choice of the number and position of regions of electron emission can promote the excitation of the desired operating mode. The transparent cathode automatically provides cathode priming.

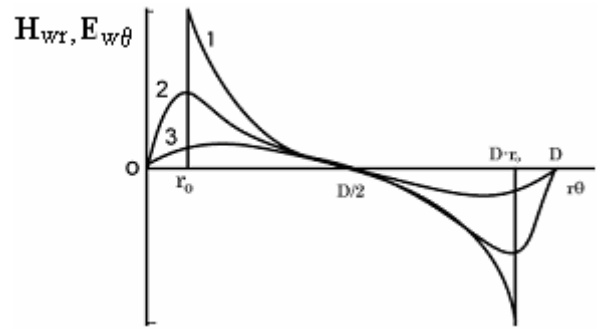


Fig.3. Distributions of azimuthal electric field and radial magnetic field of the wiggler over its period  $D$  (in arbitrary units): 1.-  $r = R_c$  (1), 2.-  $r = R_c + r_0$  (2), 3.-  $r = R_c + 2r_0$

The rate of buildup is determined by the azimuthal electric field  $E_\theta$  of the operating wave that captures electrons in a resonant system. The transparent cathode provides the fastest start of oscillations.

The transparent cathode also is a periodic slow wave structure (SWS) in the coaxial cavity that gives rise to azimuthal spatial harmonics of eigenmodes of this electrodynamic system. This is reminiscent of the nigratron [10], in which a SWS is formed by cylindri-

cal electrodes, with the cathode and anode both consisting of longitudinal rods periodically arranged on cylindrical surfaces.

### 3. Magnetron with a Transparent Cathode

In a magnetron, the azimuthal electric field of the operating wave synchronous with the rotating electron sheath is responsible for the radial drift of electrons from the cathode to the anode (which consists of a periodic resonant system). This drift is accompanied by a transfer of potential energy from electrons to the electromagnetic field. The average radial velocity of the electrons is  $v_{er} = c E_{\theta} / H_0$ . The field  $E_{\theta}$  in the electron sheath rotating around the transparent cathode is much stronger than near the solid cathode (Fig. 4). Therefore, the formation of electron spokes (Fig. 5) and an increase of microwave oscillations (Fig. 6) in a magnetron with a transparent cathode is much faster than in a magnetron with a solid cathode with uniform electron emission, and also with non-uniform emission (cathode priming [9]).

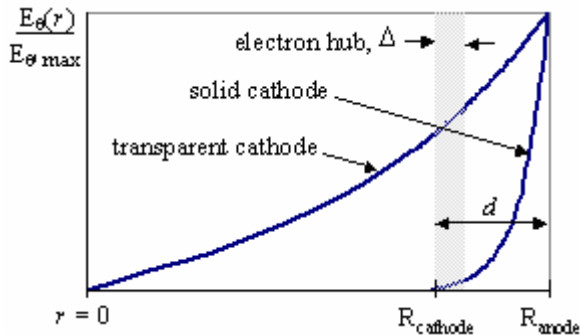


Fig. 4. Radial distributions of the wave azimuthal electric field in a magnetron with solid and transparent cathodes ( $d = R_a - R_c$ ,  $\Delta$  is a thickness of an electron sheath)

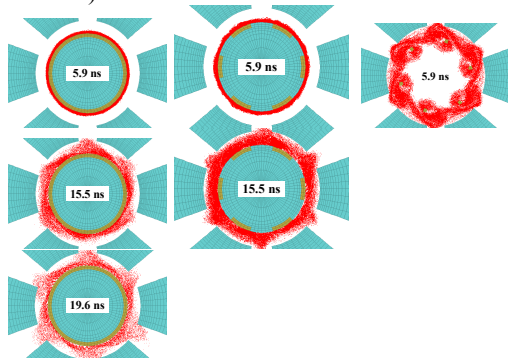


Fig. 5. Formation of electron spokes in the A6 magnetron using a solid cathode (left), cathode priming with 6 emitting regions (center), and a transparent cathode with 6 strips (right) when  $U = 350$  kV with rise time  $t_U = 10$  ns

Figs. 5 and 6 suggest that the main reason for faster start of oscillations in the magnetron is the stronger electric field  $E_{\theta}$  in the electron sheath that is provided by the transparent cathode, rather than improvement of the initial conditions achieved by cathode priming. This removes the contradiction between faster start of oscillations and improvement of the efficiency. To increase the electronic efficiency  $\eta_e$ , which characterizes the part of the electron power  $P_e = UI_a$  that is transferred to radiation power  $\tilde{P}$ ,

$$\eta_e = \tilde{P} / P_e \approx 1 - \Delta / d, \quad (4)$$

the thickness  $\Delta$  of the electron sheath should be decreased in relation to the gap  $d = R_a - R_c$  between electrodes [11].

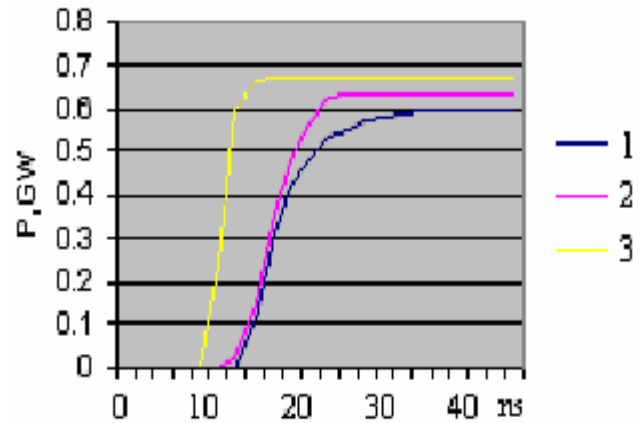


Fig. 6. Output power of the A6 magnetron with (1) a solid cathode, (2) solid cathode with cathode priming, and (3) transparent cathode when the applied voltage is  $U = 350$  kV with rise time  $t_U = 10$  ns and  $2\pi$ -mode

Higher efficiency can be achieved through a coordinated increase in the applied voltage and axial magnetic field (which saves the synchronism (3) and decreases the electron sheath thickness  $\Delta \sim U / H_0^2$ ). However, in a magnetron with a solid cathode this eventually leads to a degradation of the output characteristics [12]. The reason for this degradation is the decrease in the field  $E_{\theta}$  in the electron sheath region (Fig. 4) that is responsible for the capturing of electrons to the anode. In a magnetron with a transparent cathode the field  $E_{\theta}$  in the electron sheath is independent of its thickness (Fig. 4), which gives the possibility to decrease the start time of oscillations and increase efficiency. Values of the efficiency (from MAGIC simulations) corresponding to a correlated increase in the applied voltage and axial magnetic field, for the A6 magnetron with solid and transparent cathodes, are shown in Fig. 7.

#### 4. Free Electron Laser using a Transparent Cathode

A free electron laser in the form of a rippled field magnetron (RFM) suggested by Bekefi [13] consists of a smooth bore relativistic magnetron with additional periodic magnetic fields  $H_{\perp}$  that are transverse to the axial direction  $z$ . In essence, this is a DMI in which the periodic field  $H_{\perp}$  is produced by set of oppositely oriented permanent magnets periodically placed around the electrodes. Electrons drift around the explosively emitting cathode in this additional periodic field  $H_{\perp}$  that is primarily radial near the center of the gap between electrodes, that is, the drift is in a transverse periodic magnetic field as in conventional FEL's.

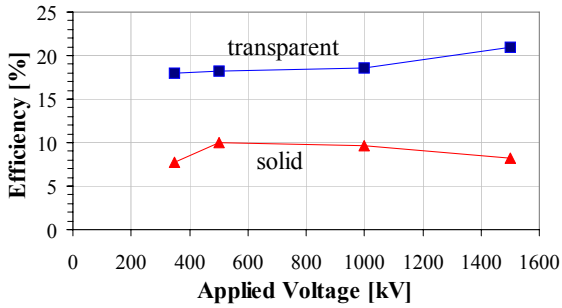


Fig. 7. Electronic efficiency for the A6 magnetron with the solid and six-strip cathodes with  $2\pi$ -mode operation

The RFM has considerable interest [14-17] as a compact oscillator capable of generating short wavelength microwaves. However, the design of this wiggler is complicated, and the requirement to use a narrow gap (otherwise the magnetic field will basically be concentrated between adjacent magnets) leads to very large unwanted axial currents in this DMI.

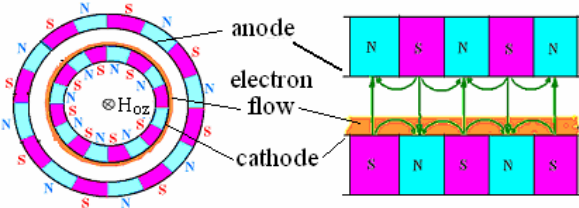


Fig. 8. A rippled-field magnetron. Right: configuration of periodical magnetic field in a RFM

We propose an FEL that also uses a DMI; however, unlike the RFM, the wiggler is the transparent cathode (Fig. 1). Such a wiggler is simpler and does not require a narrow gap. A radius of this cathode can be chosen so as to provide a suitable current. The maximum values of periodic magnetostatic and electrostatic fields occur in the region of the electron sheath, and the axial current is not useless since they produce the periodic field  $H_{\perp}$ .

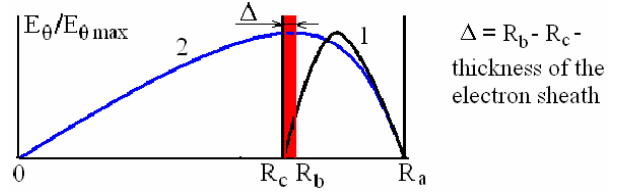


Fig. 9. Radial distributions of the azimuthal electric field  $E_{\theta}$  of a TE-mode in the RFM (1) and in the FEL with a transparent cathode (2)

As with the magnetron, such a cathode is transparent to TE modes that provide a strong azimuthal field  $E_{\theta}$  of these modes in the electron sheath unlike the RFM with a solid cathode (Fig. 9). For TM modes the  $E_{\theta}$  distribution in the FEL is as in the RFM. This means that the FEL looks like a circular cavity for the TE eigenmodes and like a coaxial cavity for the TM eigenmodes. Within the electron flow the field  $E_{\theta}$  of TE modes is almost uniform and significantly stronger than the TM ones, providing the best condition for synchronous interaction of the TE modes with electrons. At the same time, the oscillating Lorentz force  $F_z$  in the axial direction, caused by the periodic radial magnetic field  $H_r$ ,  $F_z \sim v_{\theta} H_r$ , can promote the excitation of the TM modes as well. Thus, both TE modes and TM modes can be operating modes of the FEL.

The periodical fields of the cathode-wiggler gives rise to azimuthal spatial harmonics for waves of the electron flow that can be in synchronism with eigenmodes of the electrodynamic system of the ubitron,

$$\omega = (h_{\theta} + m\bar{h})v_{e\theta}. \quad (5)$$

Here  $\omega$  is a frequency,  $\bar{h} = 2\pi/D = N/R_c$  is a constant of the wiggler with azimuthal period  $D$ ,  $m = 0, \pm 1, \pm 2, \dots$  is a number of a spatial harmonic, and  $h_{\theta} = n/R_c$  is a wave number of the operating mode with azimuthal index  $n$ . Since the spectrum of the eigenmodes in the FEL cavity is discrete,

$$\omega_n = \omega(n/R_c), \quad (6)$$

simultaneous solution of (5) and (6) is possible only for definite values of the field  $H_{0z}$ . This resonant dependence should hold even in the case where reflections from the axial ends of the wiggler are so small that the coaxial electrodynamic system behaves more like a waveguide than a cavity. The frequencies (6) are then close to the cut-off frequencies because the coupling of the quasi-transverse wave with others (including electron waves) is maximum [18], which provides the best balance between electromagnetic energy pumping by electrons and radiating waves.

Two-dimensional MAGIC simulations show the evolution of electron waves in a DMI with a transpar-

ent cathode (Fig. 10) for various values of the axial magnetic field  $H_{0z}$ . The same rotating wave structures occur in a DMI with a solid cathode (Fig. 11), as was predicted by Buneman [2]. Therefore, for the FEL these wave structures can be considered as their fundamental harmonics,  $m = 0$ . The structures in Figs. 10 and 11 were calculated without axial currents, that is, only with an electrostatic wiggler.

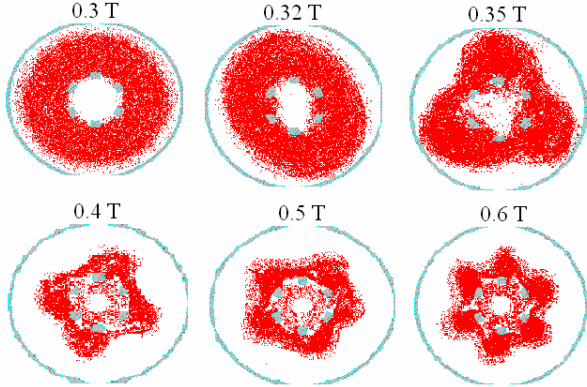


Fig. 10. Lowest structures of electron waves in DMI with a transparent cathode

Because of this, the shown structures are independent of the direction of the applied axial magnetic field.

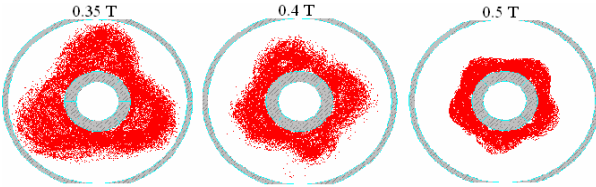


Fig. 11. Some lowest structures of electron waves in DMI with a solid cathode

As an example, for one of the resonant values of the field  $H_{0z}$ , the results of 3D MAGIC simulations for radiated power and spectrum are shown in Fig. 12. The calculated electron beam current is 3.83 kA and the efficiency is about 6 %.

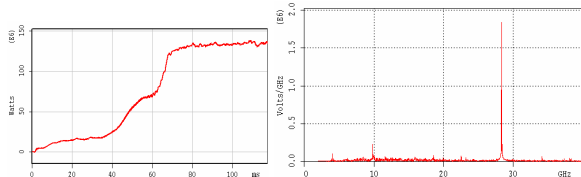


Fig. 12. Power of radiation (left) and its spectrum (right) for an FEL with an 8-strip cathode of outer radius 0.9 cm and inner radius 0.7 cm in the anode with radius 2.2 cm when  $H_{0z} = 11$  kOe and  $U = 0.6$  MV with risetime  $t_U = 1$  ns

Experiments with the crossed-field FEL were performed at the SINUS-6 high-current 3 GW electron beam accelerator (Fig. 13), which can produce a 20 ns accelerating voltage pulse up to 700 kV. We use the

8-strip graphite cathode (Fig. 14) with the inner and outer radii 6 cm and 8.5 cm, length of separate emitters 7 cm and azimuthal dimension of each emitter  $25^\circ$ . The cathode is coaxially placed up to 15 cm in a cylindrical stainless steel waveguide with radius  $R_a = 2.54$  cm and length 40 cm. The uniform axial magnetic field up to 10 kOe is provided by a 3 ms pulsed solenoid. Microwaves are radiated by the horn antenna with aperture  $a = 9$  cm through polyethylene vacuum window of diameter 25 cm.

As with the RFM, the FEL can operate at many resonant frequencies. However, the first measurements of the output radiation were limited by the frequency region 2 – 4 GHz because only an S-band receiving antenna was available for the current experiment (as antenna we use a waveguide without flange). In this range the resonance  $P(H_{0z})$  was found for  $H_{0z} = 3.2$  kOe consisting of two different radiation patterns  $P(R_\perp)$ , shown in Fig. 16: a pattern corresponding to the  $TE_{11}$  mode with the frequency  $f = 3.1$  GHz, and a pattern with the minimum radiation in the center with  $f = 3.7$  GHz.

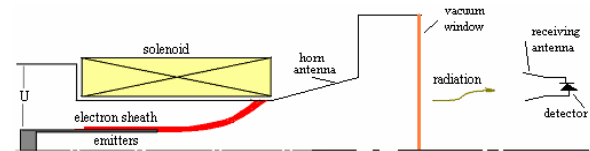


Fig. 13. Schematic of experimental set up for the FEL

Pulses of the applied voltage, total axial electron beam current and microwave signal (in Fig. 17 five microwave pulses are overlaid) were observed using a capacitor divider, Rogowski coil and a crystal detector, respectively.

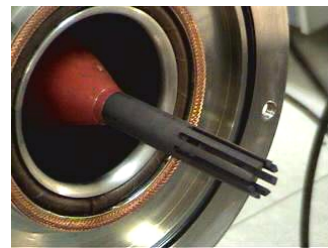


Fig. 14. Photo of the 8-emitter graphite cathode



Fig. 15. Photo of the output antenna and vacuum window of the SINUS-6 accelerator

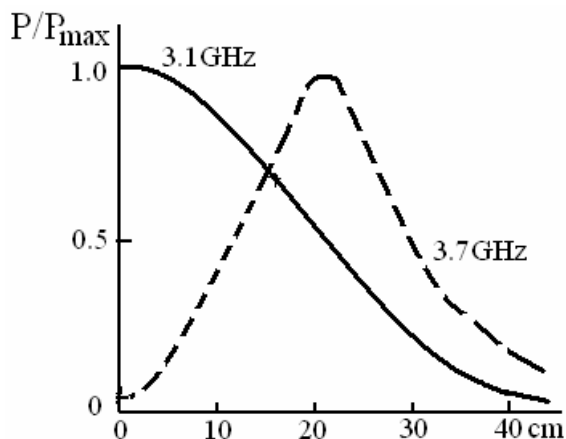


Fig. 16. Radiation pattern observed at a distance 1.5 m from the horn antenna with aperture 9 cm

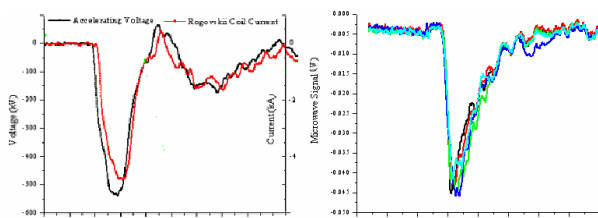


Fig. 17. Pulses of the applied voltage from the capacitance divider, electron beam current from the Rogowski coil and microwaves from the crystal detector with 60 dB attenuator

Microwaves were measured at a distance  $L = 1.5$  m from the radiating horn antenna aperture, that is, in the far zone (Fresnel's parameter  $L\lambda/a^2 \gg 1$ ) where the reactive fields of the radiating antenna, as well as longitudinal wave field components, vanish. Radiation power for each symmetrical radiation pattern was estimated as  $P_1 \approx P_2 \approx 2$  MW. However, radiation from the FEL propagates through the uniform stainless steel waveguide (Fig. 13) where the cut-off frequency of the  $TE_{11}$ -mode  $f_{cut-off} = 3.4$  GHz exceeds the measured radiation frequency  $f = 3.1$  GHz. That is, we measure the evanescent tail of the radiated power. In future experiments we plan to change the configuration of the channel to correct for this situation, and to prepare diagnostics to find and measure other resonances with shorter wavelengths.

## Conclusions

Particle-in-cell computer simulations using the MAGIC code have demonstrated that use of the transparent cathode instead of a solid cathode brings improved performance to cross-field devices. The improved performance is attributed to i) a stronger azi-

muthal wave electric field at the location of the electron sheath compared to a solid cathode, ii) bunching effects attributed to both cathode and magnetic priming, and iii) the effects of a periodic electrostatic wiggler. Plans are underway to experimentally test these using an A6-type magnetron with extraction output. The transparent cathode also naturally manifests as novel M-type FEL, with radiation parameters controlled by the applied axial magnetic field. This is a promising microwave source for many applications owing to its simple design. Preliminary experimental results have been presented.

## References

- [1] M.I. Fuks, *Sov. Phys. Tech. Phys.*, vol. 27, 432, 1982.
- [2] O. Buneman, in E. Okress, Ed., *Crossed-Field Microwave Devices*, Academic Press, New York, 1, 209, 1961.
- [3] M.C. Clark, B.M. Marder, and L.D. Bacon, *Appl. Phys. Lett.*, vol. 52, 78, 1988.
- [4] M.Fuks and E.Schamiloglu, *Phys. Rev. Lett.*, vol. 95, 203101, 2005.
- [5] M. Fuks and E. Schamiloglu, 2006 IEEE Int. Vacuum Electronics Conf., 283, 2006.
- [6] B. Goplen, L. Ludeking, D. Smithe and G. Warren, *Comp. Phys. Comm.*, vol. 87, 54, 1995.
- [7] V.B. Neculaes, R.M. Gilgenbach, and Y.Y. Lau, *Appl. Phys. Lett.*, vol. 83, 1938, 2003.
- [8] G.B. Collins, Ed., "Microwave magnetrons," McGraw-Book Company, New York, 1948.
- [9] M.C. Jones, V.B. Neculaes, Y.Y. Lau, R.M. Gilgenbach, and W.M. White, *Appl. Phys. Lett.*, vol. 85, 6332, 2004.
- [10] P.L. Kapitsa, "High Power Electronics," vol. 7, AS USSR, Moscow, 1962 (in Russian).
- [11] V.E. Nechaev, M.I. Petelin, and M.I. Fuks, *Sov. Tech. Phys. Lett.*, vol. 3, 310, 1977.
- [12] L.A. Weinstein and V.A. Solntsev, "Lectures on HF Electronics," Moscow, Sov. Radio, 1973 (in Russian).
- [13] G. Bekefi, *Appl. Phys. Lett.*, vol. 40, 578, 1982.
- [14] G. Bekefi and R.E. Shefer, *Appl. Phys. Lett.*, vol. 44, 280, 1984.
- [15] C.L. Chang, E. Ott, T.M. Antonsen, Jr., and A.T. Drobot, *Phys. Fluids*, vol. 27, 2937, 1984.
- [16] W.W. Destler, F.M. Aghamir, D.A. Boyd, G. Bekefi, R.E. Shefer, and Y.Z. Yin, *Phys. Fluids*, vol. 28, 1962, 1985.
- [17] F. Hartemann, G. Bekefi and R.E. Shefer, *IEEE Trans. Plasma Sci.*, vol. 13, 484, 1985.
- [18] B.Z. Katsenelenbaum, L. Mercader del Rio, M. Pereyaslavets, M. Sorola Ayza, and M. Thumm, "Theory of Nonuniform Waveguides," The Institute of Electrical Engineers, London, UK, 1998.